Spatiotemporal dynamics of termite infestation in urban *Araucaria cunninghamii*: A case study in Taipei

*Cheng-Jung Lin**
Senior Researcher
Forest Products Utilization Division, Taiwan Forestry Research Institute
53 Nanhai Rd., Taipei 10066, Taiwan
zzlin@tfri.gov.tw

Bing-Syun Peng
Associate Researcher
Chiayi Research Center, Taiwan Forestry Research Institute
53 Nanhai Rd., Taipei 10066, Taiwan
bspeng@tfri.gov.tw

*Po-Heng Lin**
Assistant Researcher
Forest Products Utilization Division, Taiwan Forestry Research Institute
53 Nanhai Rd., Taipei 10066, Taiwan
afarmer@tfri.gov.tw

Chieh-Yu Chang
Assistant
Forest Products Utilization Division, Taiwan Forestry Research Institute
53 Nanhai Rd., Taipei 10066, Taiwan
cychang@tfri.gov.tw

(Received 19 March 2025)

Abstract. Termite feeding on the trunk cross-sections of *Araucaria cunninghamii* in Taipei, Taiwan, was examined using 2D stress wave imaging (FAKOPP system). Six inspections were conducted at 2-month intervals to monitor six trees. 2D cross-sectional stress wave velocity images were created at different heights (30–180 cm) to assess termite feeding damage. Termite damage, quantified as damage ratio (DR, %), ranged from 0% to 55% across different trees and heights, with maximum increases of up to 21% in DR observed over a 2-month period. In the investigated cases, termites primarily fed on the interior of tree trunks. The feeding pattern typically extended longitudinally, then proceeded in a tangential (circular) direction, and finally moved radially. This study identified *Coptotermes formosanus* as a key termite species involved. Typically, termites prioritized feeding on the earlywood over the latewood. The periods with the highest damage to trunk cross-sections due to termite feeding occurred during seasons with higher temperatures and relative humidity. Damage initially appeared near the heartwood or the boundary between the heartwood and sapwood, gradually expanding into the heartwood. Of the six trees monitored for the full study duration (after one tree was felled for validation), subterranean termite tunneling was observed as the primary pattern in three trees, while aerial swarm invasion patterns were inferred for two trees based on initial damage locations.

Keywords: Termite; Feeding behavior;Visual tree assessment; Nondestructive technique; *Coptotermes formosanus; Araucaria cunninghamii*

Introduction

Termites are integral to ecosystems, contributing to processes like nutrient cycling and decomposition (Myer and Forschler 2018), but certain species, particularly wood-feeders, simultaneously present potential threats to forest ecology and trees. Certain termite species, such as those belonging to the genus *Coptotermes*, are notorious for their wood-feeding habits, with a particular inclination for devouring the interiors of living trees, posing significant risks to their structural integrity. This propensity poses a substantial risk to both the structural stability and overall health of trees. Therefore, a comprehensive exploration of termite behavior and their potential tree-related damage is important for assessing risk.

In Taiwan, hoop pine (*Araucaria cunninghamii* Aiton ex D. Don.) is commonly planted as an ornamental tree in parks,

* Corresponding author

roadsides, and campuses throughout Taipei due to its aesthetic appeal and adaptability to urban environments. While multiple tree species in Taipei are susceptible to termite attack, recent incidents involving *A. cunninghamii* on the study campus highlighted a specific vulnerability that warranted focused investigation. Recent research has underscored the susceptibility of hoop pines to termite-induced damage, often culminating in unanticipated tree collapse (Lin et al. 2016). Such collapses can pose significant threats to human safety and property, given that termite-infested trees frequently become unstable because of damage to their trunk bases and main stems. In Taiwan, termites from the *Coptotermes* genus, notably the Formosan subterranean termite (*Coptotermes formosanus* Shiraki), are recognized as major contributors to forest and tree deterioration (Liang et al. 2020). Surveys reveal that, following tree damage caused by typhoons, these termites target the heartwood of standing tree trunks, resulting in hollowing and structural impairment within the stem (Lai 2019).

The assessment and management of tree-related risks are critical for upholding the safety and well-being of forests and individual trees. In forest resource management, early detection and appraisal of potential hazards play a key role in averting damages and ensuring the long-term viability of forests. Consequently, the realms of tree risk assessment and management have acquired considerable importance. Heightened concerns about public safety and the preservation of urban trees have accentuated the need for the development and application of rapid, precise, and cost-effective technologies to identify decay and other structural vulnerabilities within trees (Li et al. 2022; Martiansyah et al. 2022).

While visual tree assessment has long been a valuable tool involving the visual inspection of external tree defects, instrumental measurement of internal flaws, and assessment of wood strength, it often falls short in detecting termite-induced damage within tree trunks, where these insects primarily operate. In response, non-destructive testing techniques employing 2D imaging methods have been developed for the assessment and examination of wooden materials. Acoustic techniques have proven highly effective for detecting and evaluating decay and voids within various tree trunks, offering a vital means of ensuring tree safety and health (Allison et al. 2020; Goh et al. 2018; Linhares et al. 2021; Soge et al. 2021). Stress wave testing, which detects internal defects by measuring the velocity of mechanical waves propagated through the trunk, has emerged as a powerful tool for assessing the internal condition of trees. Termite-damaged areas, containing internal voids or decayed wood, typically exhibit reduced stress wave velocity compared to sound wood, allowing for their detection and mapping (Lin et al. 2016; Wei et al. 2022). The non-invasive nature of stress wave and ultrasonic assessments makes them practical and feasible for tree inspections.

Selection of *A. cunninghamii* as the subject of this research arises from the discovery of termite infestation by *C. formosanus*, commonly referred to as the Formosan subterranean termite, within this tree species on the campus of a university in Taipei. The presence of termite colonies within these trees carries long-term implications. However, quantitative *in situ* monitoring of subterranean termite feeding in urban trees remains challenging (Thant et al. 2022), meaning that for these specific trees, the rate and extent of termite feeding remain unclear. To systematically monitor and manage these trees, a detailed program of inspections and analyses is indispensable. Our principal objective is to acquire an extensive understanding of termite invasion patterns, as well as the rates and patterns of damage inflicted by termites on the internal wood of *A. cunninghamii* trees. To achieve this objective, we monitored termite activity in *A. cunninghamii* using non-destructive 2D stress wave imaging at multiple time points (six inspections at 2-month intervals) and tree heights (30–180 cm). This approach allowed us to detect and assess termite feeding behavior, shedding light on termite invasion patterns and the extent of their internal damage. The outcomes of this research endeavor will provide invaluable insights for tree risk assessment and management, while also contributing to strategies for the prevention and control of termite infestations

Materials and methods

Materials

This study was conducted within the Gongguan Campus of National Taiwan Normal University (NTNU, 25.00790°N, 121.53711°E), in Taipei, Taiwan. The background for this research stems from an incident that occurred in April 2022 when an *A. cunninghamii* tree collapsed on the campus. Subsequent examination of the internal tree trunk revealed damage caused by the Formosan subterranean termite (*C. formosanus*). To ensure the safety of all *A. cunninghamii* trees on the campus, a comprehensive survey was carried out in the immediate vicinity (within a 50-m radius) of the fallen tree to identify trees that might have been affected by termite infestation. This survey involved visual inspection for external signs of termite activity (e.g., mud tubes, damaged bark) and preliminary stress wave screening on approximately 15 *A. cunninghamii* trees in this zone. The initial goal was to establish a tree risk monitoring and management system. Selection criteria included: (1) proximity

to the original collapsed tree, (2) presence of preliminary signs of potential termite activity or internal defects suggestive of infestation based on the initial screening, and (3) accessibility for repeated measurements. The selected trees represented a range of conditions observed in the affected area. Given the presence of termite populations in the region and their potential for ongoing harm to the trees, it became necessary to conduct regular inspections of these trees to gain a deeper understanding of the invasion patterns and rates of internal termite damage.

Stress wave tomography and damage assessment

To evaluate the extent of termite feeding damage, we conducted experimental inspections on all the trees in the vicinity of the fallen tree. We selected six *A. cunninghamii* trees for long-term monitoring of termite feeding damage. Trees ranged in age from 40 to 50 years and had a breast height diameter ranging from approximately 40 to 55 cm. Considering that termite infestations primarily occur inside trees, we employed stress wave detection methods (Figure 1). Tests were conducted in June 2022, August 2022, October 2022, December 2022, February 2023, and April 2023, to examine the cross-sectional trunk areas at different height levels and assess the extent of termite damage within the trees.

We employed a FAKOPP stress wave timer (FAKOPP Enterprise, Hungary) equipped with eight probes. Measurements were taken at eight equidistant points along the circumference of the tree trunk approximately 30, 60, 90, 120, 150, and 180 cm in height from the ground along the tree trunk, targeting sections with visible or suspected signs of termite infestation (e.g., mud tubes on bark, flight holes, galleries exposed after minimal bark removal, or hollow sounds upon tapping) and areas suspected of containing decay cavities based on preliminary visual assessments or an initial campus-wide survey.

The sensors were oriented perpendicular to the longitudinal axis of the tree trunk to measure the propagation time and stress wave velocity. We conducted the strikes in sequential order at positions 1 to 8, repeating the measurements five times to obtain an average value. Throughout the testing process, we acquired a complete data matrix for the transverse stress wave detection area of each tree. Each probe act sequentially as a transmitter while the remaining seven acted as receivers. The number of unique pairwise paths for stress wave propagation was calculated as $N(N-1)/2$, where N is the number of probes. Thus, eight probes resulted in $(8\times7)/2=28$ independent propagation time measurements at each test location. The propagation path of the transverse stress wave was determined by utilizing the eight probes with both receiving and transmitting capabilities.

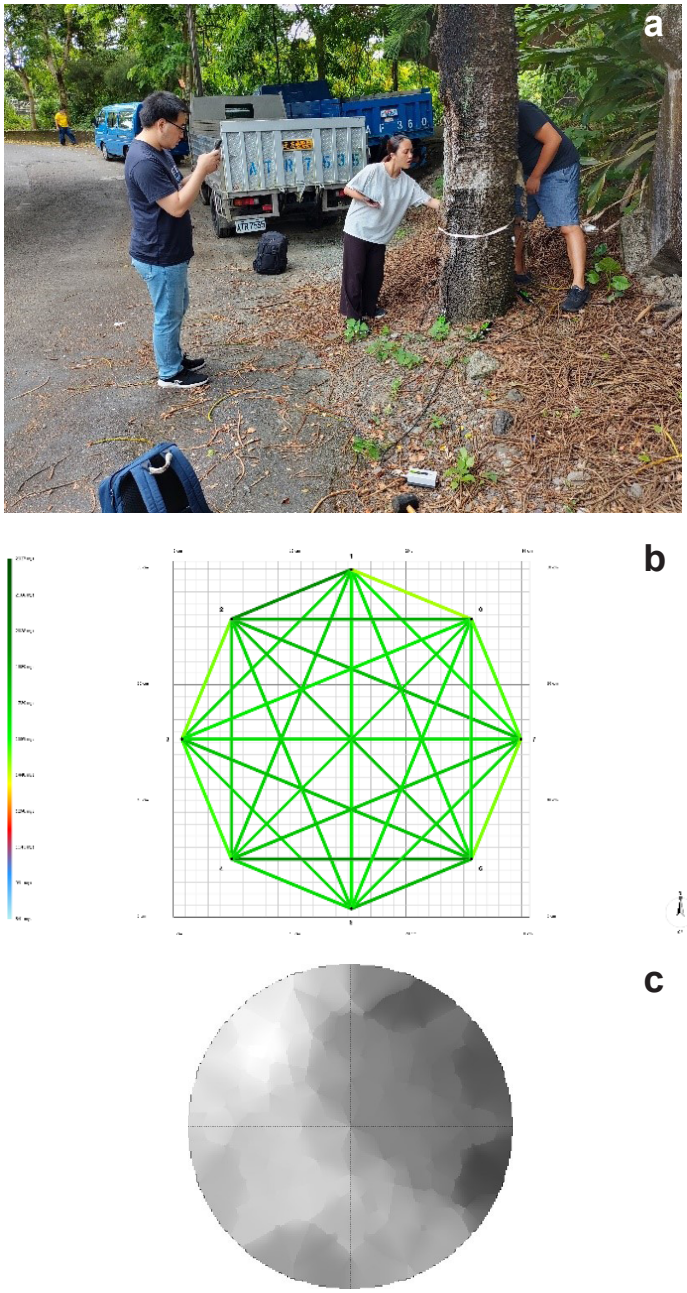

Figure 1. Acoustic tomography test on *A. cunninghamia* trees using a Fakopp stress wave tomographic tool showing (a) the sensor arrangement; (b) the paths of acoustic measurement; and (c) a grayscale image of a stress wave tomogram.

Data analyses

The cross-sections and the distances between sensors were measured with a tape measure. The software approximated the circular cross-sectional shape as the standard. All instruments were operated according to their respective operational manuals, with data computation and analysis performed using the ArborSonic software. Although raw propagation times were collected, the software internally used these times along with

precise path distances (derived from the input geometry) to generate velocity values. Concurrently, the influence of probe spacing was also handled internally by the software; thus, velocity values were inherently normalized by the software.

First, following the completion of stress wave acoustic measurements, we employed ArborSonic software to generate transverse stress wave 2D images for each cross-section. Each 2D stress wave image was accompanied by a color scale that represented the measured stress wave velocity. The scale was calibrated separately for each sample tree so that its endpoints corresponded to the maximum and minimum velocities recorded during that particular test. Secondly, we used the ArborSonic software program to generate stress wave velocity 2D images of the cross-sections, which were calculated based on the raw, unadjusted, and unnormalized propagation times obtained during the experiments.

The stress wave velocity corresponding to each pixel in the images was quantitively used to assess stress wave velocity in 2 D images. Visualization and transformation of the 2D cross-sectional images were used to generate stress wave velocity distribution maps for different positions. Each 2D stress wave image was accompanied by a color scale that represented the measured stress wave velocity. The scale was calibrated separately for each sample tree so that the endpoints corresponded to the maximum and minimum velocities recorded during that particular test. Finally, we rationalized and corrected the damage rate of termite feeding on the trunk cross-sections based on the 2D images. According to the operating manual, the damage ratio (DR, %) was operated such that when the relative velocity decrease was 0, 5, 10, 15, 20, 30, 40, 50, and >50%, the estimated decayed area was 0, 0, 0, 0–10, 10–20, 10–20, 20–40, 30–50, and >50% by ArborSonic software, respectively (FAKOPP 2020).

Gross errors or noisy signals were managed according to the operator manual guidelines, and re-measurements were performed at that sensor point. Multiple stress wave measurements were repeated at each probe to collect five data points, which were then averaged to provide a mean propagation time for each path before velocity calculation. The variability of these repeated measurements was monitored during collection to ensure signal stability.

After integrating the stress wave characteristic information and 2D images of each cross-section, we conducted sampling using an increment borer to extract 5 mm diameter increment cores from the bark to the pith of each tree trunk. The cores were assessed for wood damage and the holes were examined using an endoscope (model TON-666LNP, resolution 370,000 pixels, with built-in LED illumination, inspection depth up to 115 cm) for signs of wood decay, damage, termites, or termite mud tunnels. This inspection served as a basis for comparison and adjustment against the stress wave velocity 2D images.

Ultimately, we chose six *A. cunninghamii* trees that had experienced termite feeding damage to be monitored over the long term. Tree No. 36 was felled in September 2022, prior to the end of the test. This tree was chosen for felling because internal stress wave assessments showed that it had consistently high and widespread internal damage and was identified as a high-risk tree by campus management, necessitating its removal (Figure 2). Finally, based on the results of the aforementioned experiments, we evaluated and summarized the patterns of termite feeding damage inside the trees. Using the adjusted termite feeding damage rates on cross-sections, we provided a reference for tree inspection and risk management.

Results and discussion

Temporal patterns of termite activity

The August 2023 examinations utilizing increment borers and endoscopic tools unveiled ongoing termite activity within Trees 29 and 32, implying that termites were actively feeding on the wood within these trees. Furthermore, although termites were not observed in Trees 28, 34, and 43, traces of termite tunneling soil, such as termite galleries partially filled with soil and frass (termite tunneling soil), were detected. These findings suggested that termites had previously been active within these trees but had gradually vacated during our inspections.

Stress wave testing of Tree 29 yielded lateral stress wave 2D images, with specific findings presented in Table 1. There was a progressive manifestation of termite activity within the tree trunk from June 2022 to April 2023, primarily originating from the base of the tree below ground level and advancing upward. Damage levels within trunk cross-sections at various heights ranged from 5% to 20%, exhibiting a gradual upward trend. Particularly noteworthy was the period between February 2023 and April 2023, where damage rates surged from 13% to 20%, representing a 7% increase in 2 months. In contrast, damage rates increased at a slower pace during other periods.

Spatial dynamic of termite damage

Tree 28 exhibited an upward termite infestation pattern, likely originating from subterranean activity, with DR ranging from 3% to 17% in the lower trunk sections (Table 2). The primary increase in damage (from 11% to 17% at 30 cm) occurred between June and August 2022. Live termites were not detected by August 2023.

Figure 2. Cross-sections of *A. cunninghamia* tree (No. 36) damaged by termite infestation.

Lateral stress wave 2D images for Tree 32 showed a gradual consumption of the tree trunk by termites (Table 3), likely originating from the base of the tree within the soil below ground level and extending upwards. Consequently, the damage rate in the trunk cross-sections near the base of the tree exceeded that at higher cross-sections. Overall, damage rates within the trunk cross-sections ranged widely, from 10% to 55%. The most substantial change transpired between August 2022 and October 2022, as the damage rate more than doubled from 16% to 37%. Thereafter, damage rates stabilized, suggesting that termites primarily consume sections that had already sustained damage.

Vertical and radial patterns of termite infestation

The stress wave 2D images for tree numbers 28, 29, and 32 consistently demonstrated termite infestation commencing near the base, close to ground level, and subsequently extending upwards. This attack often commenced in the heartwood or at the heart/sap boundary before progressively infiltrating the heartwood region.

Stress wave 2D images for Tree 34 showed gradual termite infestation within the tree trunk where damage was initially observed or was more concentrated in the upper portions of the assessed trunk sections and appeared to extend downwards towards the base (Table 4). Overall, damage rates within the trunk cross-sections varied from 7% to 29%. The most notable change occurred between August and October 2022, with the damage rate escalating from 23% to 31%. Subsequently, there was a modest rise (ranging from 2% to 5%) in damage rates across various trunk cross-sections during later inspection periods.

In line with inspection results, termite infestation initially emerged 1.5 m above the ground, infiltrating the trunk cross-section from the outer side at the juncture of the sapwood and

Table 1. Transversal stress wave velocities and 2D imaging of *A. cunninghamii* (Tree No. 29) 30 cm above ground, based on six time-series sampling points collected from June 2022 to April 2023.

No	Tree height (cm)	Velocity (m/sec)	June 2022	August 2022	October 2022	December 2022	February 2023	April 2023
29	30	Max	1264	1214	1289	1312	1320	1261
		Min	967	928	986	1004	1009	964
2D			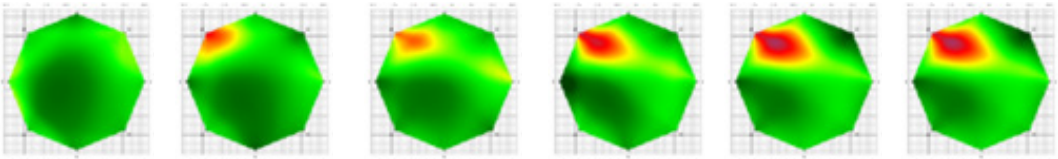					
DR (%)			0	5	6	10	13	20

DR, damage ratio (%)

Table 2. Transversal stress wave velocities and 2D imaging of *A. cunninghamii* (Tree No. 28) 30, 45 and 60 cm above the ground, based on six time-series sampling points collected from June 2022 to April 2023.

No	Tree height (cm)	Velocity (m/sec)	June 2022	August 2022	October 2022	December 2022	February 2023	April 2023
28	60	Max	1384	1337	1342	1376	1379	1342
		Min	1059	1023	1026	1052	1055	1026
2D			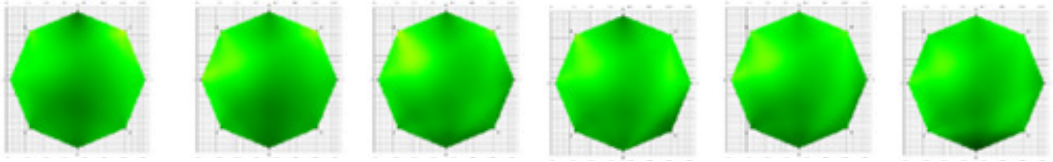					
DR (%)			0	0	0	0	0	0
28	45	Max	1331	1344	1294	1344	1314	1272
		Min	1018	1028	989	1028	1005	973
2D			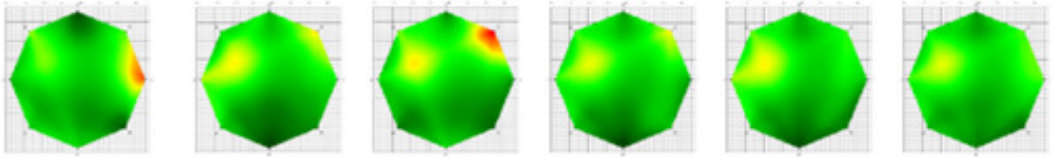					
DR (%)			3	3	4	4	4	4
28	30	Max	1195	1303	1252	1266	1308	1235
		Min	914	997	958	968	1000	945
2D			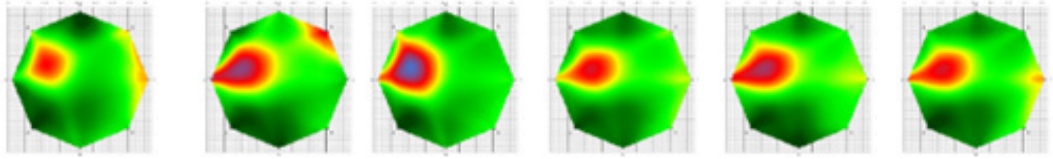					
DR(%)			11	17	17	17	17	17

DR, damage ratio (%)

heartwood, and gradually progressing towards the base and heartwood. The trunk sections 90 cm and 120 cm above the ground sustained the most substantial impact.

Stress wave 2D images for Tree 43 revealed gradual termite infestation within the tree trunk, potentially emanating from the upper sections and descending towards the base (Table 5). Overall, damage rates within the trunk cross-sections ranged from 7% to 35%. The most remarkable transition occurred between February and April 2023, with damage rates rising from 14% to 19%. Rates ranging from 2% to 4% were

Table 3. Transversal stress wave velocities and 2D imaging of *A. cunninghamii* (Tree No. 32) 30, 60, 90, 120 and 150 cm, based on six time-series sampling points collected from June 2022 to April 2023.

No	Tree height(cm)	Velocity (m/sec)	June 2022	August 2022	October 2022	December 2022	February 2023	April 2023
32	150	Max	1643	1556	1472	1571	1640	1542
		Min	1257	1190	1126	1201	1254	1180
2D			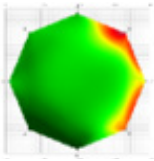	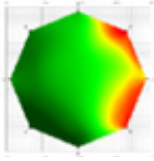	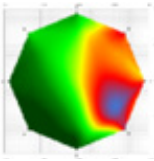	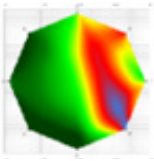	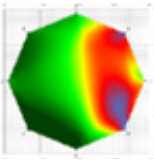	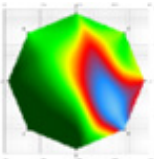
DR (%)			10	16	37	37	37	37
32	120	Max	1258	1158	1105	1157	1131	1109
		Min	962	886	845	885	865	848
2D			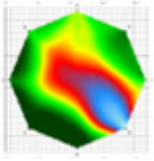	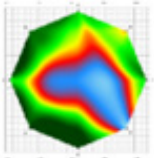	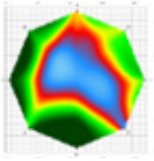	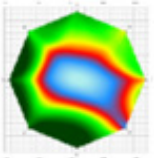	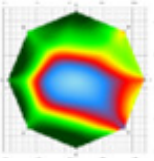	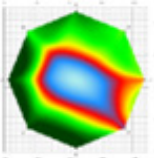
DR (%)			40	48	52	52	52	52
32	90	Max	1366	1198	1221	1236	1182	1180
		Min	1045	916	933	945	904	902
2D			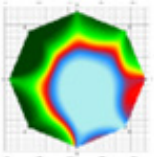	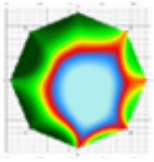	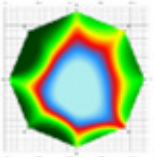	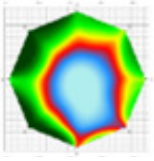	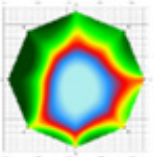	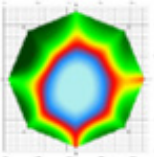
DR (%)			54	54	54	54	54	54
32	60	Max	1406	1325	1170	1276	1384	1315
		Min	1076	1013	895	976	1059	1005
2D			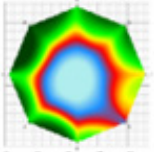	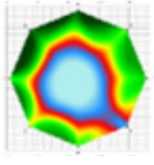	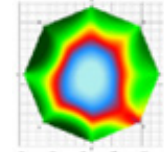	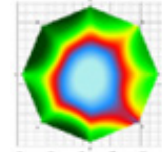	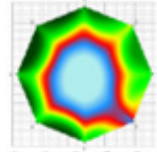	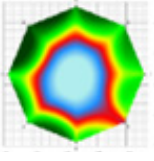
DR (%)			54	54	54	54	54	54
32	30	Max	1042	1002	1027	993	1026	996
		Min	797	766	785	760	785	762
2D			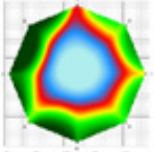	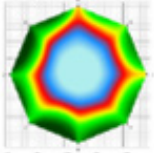	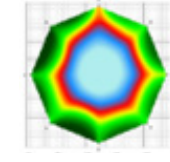	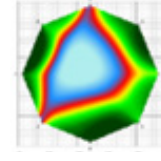	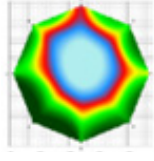	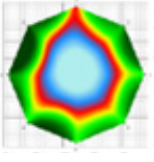
DR (%)			55	55	55	55	55	55

DR, damage ratio (%)

Table 4. Transversal stress wave velocities and 2D imaging of *A. cunninghamii* (Tree No. 34) 30, 60, 90, 120 and 150 cm, based on six time-series sampling points collected from June 2022 to April 2023.

No	Tree height (cm)	Velocity (m/sec)	June 2022	August 2022	October 2022	December 2022	February 2023	April 2023
34	150	Max	1571	1548	1519	1486	1509	1563
		Min	1202	1184	1161	1136	1154	1195
2D			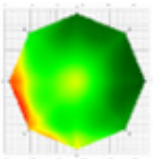	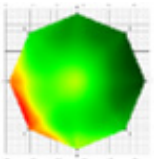	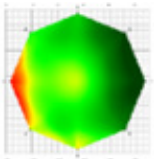	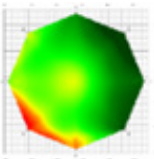	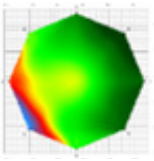	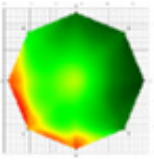
DR (%)			7	8	8	8	13	13
34	120	Max	1459	1440	1449	1387	1408	1429
		Min	1116	1101	1108	1061	1076	1093
2D			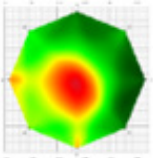	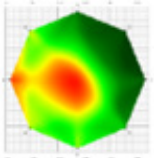	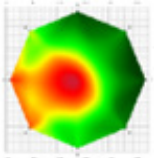	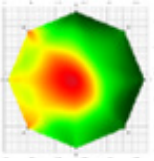	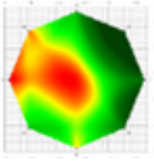	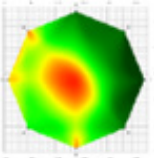
DR (%)			21	23	31	31	31	31
34	90	Max	1373	1452	1440	1438	1453	1443
		Min	1050	1110	1101	1099	1111	1104
2D			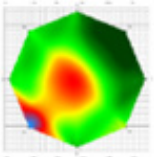	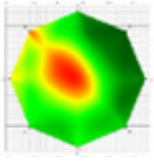	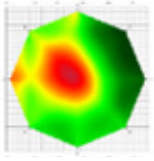	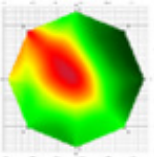	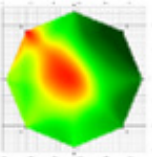	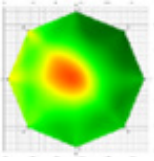
DR (%)			25	25	25	29	29	29
34	60	Max	1381	1434	1417	1416	1403	1392
		Min	1056	1097	1083	1083	1073	1064
2D			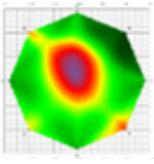	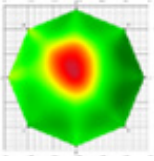	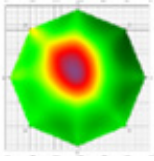	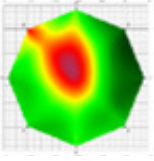	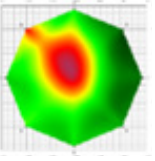	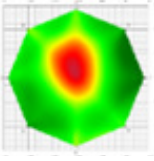
DR (%)			20	20	20	24	24	24
34	30	Max	1352	1397	1400	1362	1307	1335
		Min	1034	1068	1071	1041	999	1021
2D			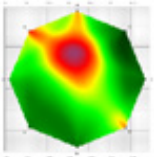	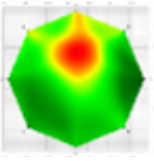	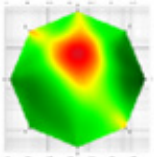	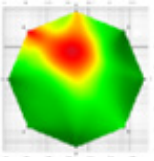	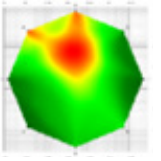	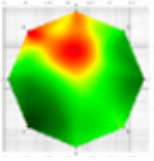
DR (%)			17	17	17	22	22	24

DR, damage ratio (%)

Table 5. Transversal stress wave velocities and 2D imaging of *A. cunninghamii* (Tree No. 43) 30, 60, 90, 120, 150 and 180 cm, based on six time-series sampling points collected from June 2022 to April 2023.

No	Tree height (cm)	Velocity (m/sec)	June 2022	August 2022	October 2022	December 2022	February 2023	April 2023
43	180	Max	1505	1513	1487	1497	1497	1475
		Min	1151	1157	1137	1144	1145	1128
2D			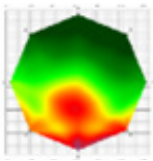	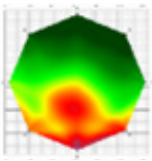	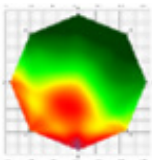	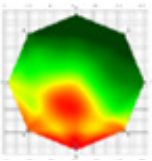	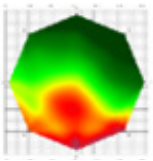	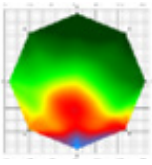
DR (%)			31	33	35	35	35	35
43	150	Max	1458	1526	1468	1537	1459	1466
		Min	1115	1167	1122	1176	1116	1121
2D			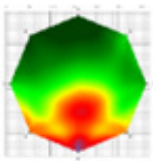	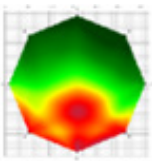	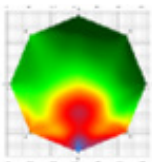	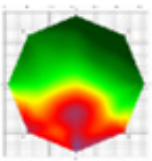	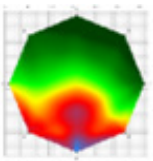	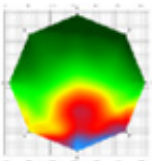
DR (%)			29	31	31	35	35	35
43	120	Max	1416	1432	1376	1428	1397	1348
		Min	1083	1095	1052	1092	1069	1031
2D			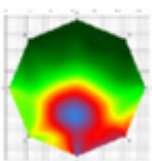	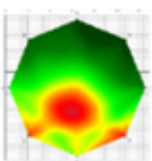	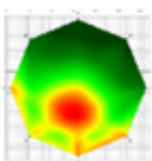	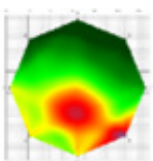	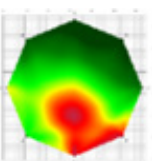	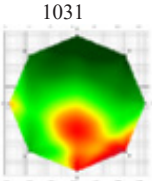
DR (%)			25	25	25	28	28	28
43	90	Max	1189	1228	1267	1373	1245	1326
		Min	909	939	969	1050	952	1014
2D			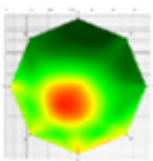	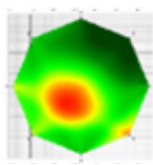	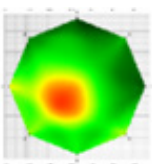	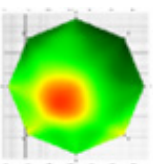	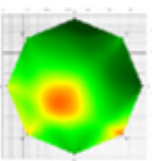	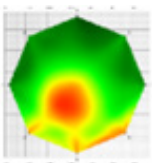
DR (%)			14	14	14	14	14	19
43	60	Max	1373	1370	1334	1384	1323	1358
		Min	1050	1048	1020	1058	1012	1038
2D			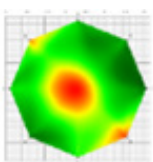	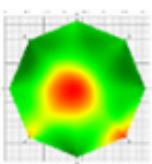	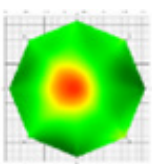	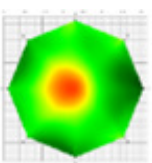	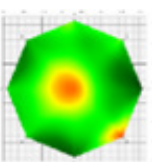	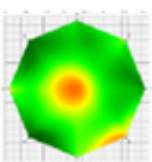
DR (%)			11	11	11	11	11	11
43	30	Max	1273	1245	1259	1302	1265	1273
		Min	974	952	963	996	968	973
2D			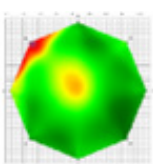	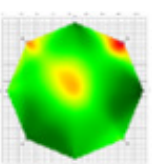	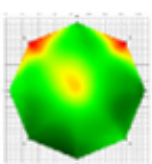	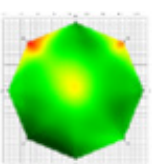	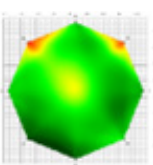	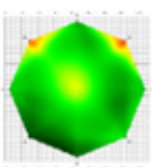
DR (%)			7	7	7	7	7	7

DR, damage ratio (%)

observed across various trunk cross-sections during different inspection periods.

Termite infestation initially occurred at 1.8 m above the ground. Trunk sections 180 cm and 150 cm above the ground experienced the most substantial impact, with higher damage rates in the upper trunk portions compared to the base.

Stress wave 2D images of Tree 36 were based on the inspections conducted in June and August 2022, before this tree was felled in September 2022 (Table 6). A visual examination was performed to assess the extent of termite damage across trunk cross-sections at varying heights (Figure 2). Visual inspection of the felled tree cross-sections allowed for detailed characterization and quantitative assessment of termite-induced damage patterns and rates (Table 6), which served to validate and calibrate the interpretation of the non-destructive stress wave data.

Visual observations indicated that termite feeding patterns involved longitudinal extension from the base upwards, followed by a tangential shift towards the earlywood, and subsequent radial movement. Termite movement patterns tended to be random, with no particular orientation. Notably, earlywood segments were the prime target of termite activity, with earlywood exhibiting more pronounced damage compared to latewood.

Termite feeding areas in Tree 36 were circular, point-like, or clustered in regions that gradually expanded and concentrated within the trunk interior. Lateral stress wave 2D images primarily detected stress wave connection signals outside the feeding areas, which served as effective evaluation indicators. Termite feeding areas were less frequent within the sapwood region and primarily manifested within the heartwood and the boundary zone between the earlywood and latewood, extending deeper into the heartwood interior. Examination of trunk cross-sections from the felled tree highlighted a noticeable water staining phenomenon in the wood surrounding the damaged areas due to termite-induced damage.

Termites in Taiwan, including species such as *Odontotermes formosanus* (Shiraki), *C. formosanus*, and *Coptotermes gestroi* (Wasmann), are recognized as significant forest pests (Lee et al. 2011) and are known to construct mud tubes on tree bark and cause feeding damage to the living tree trunk. It is important to distinguish their feeding behaviors. For instance, *O. formosanus* primarily constructs mud tubes on the surface of tree trunks and feeds on the tree bark covered by these tubes, without invading the tree interior. In contrast, species like *C. formosanus*, identified in our study, are known to cause

Table 6. Transversal stress wave velocities and 2D imaging of *A. cunninghamii* (Tree No. 36) 30, 60, 90, 120, 150 and 180 cm, based on six time-series sampling points collected from June 2022 to August 2022.

No	Tree height (cm)	Velocity (m/sec)	June 2022	August 2022
36	30	Max	1452	1434
		Min	1110	1097
2D			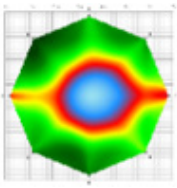	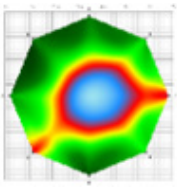
DR (%)			38	38
36	60	Max	1520	1443
		Min	1162	1104
2D			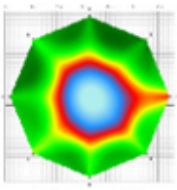	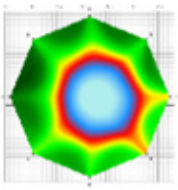
DR (%)			37	41
36	90	Max	1463	1427
		Min	1119	1091
2D			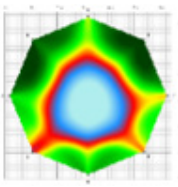	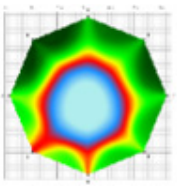
DR (%)			47	47
36	120	Max	1447	1292
		Min	1106	988
2D			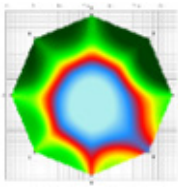	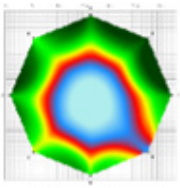
DR (%)			51	51
36	150	Max	1563	1438
		Min	1195	1100
2D			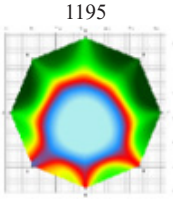	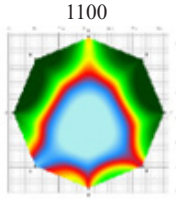
DR (%)			53	56
36	180	Max	1557	1456
		Min	1191	1114
2D			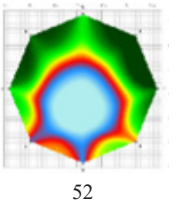	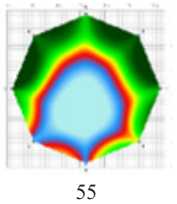
DR (%)			52	55

DR, damage ratio (%)

extensive internal damage. Chiu et al. (2020) observed that trees were primarily affected by *O. formosanus*, with varying infestation rates among different tree species associated with distinct tree characteristics. This highlights the potential for different termite species to dominate in different contexts or tree species, exhibiting varied impacts.

The aggressive feeding behavior of *Coptotermes* species significantly impacts tree health. For instance, mud tubes built by *C. gestroi* can extend as high as 6.35 m above ground on dead trunks of Luchu pine (*Pinus luchuensis* Mayr.), with 16.0% of the cross-sectional areas of the trunk being damaged by feeding. Lin et al. (2021) suggested that the feeding damage patterns of *C. gestroi* and *C. formosanus* are similar, as they tunnel into the trunk and base of trees, increasing their susceptibility to collapse. Furthermore, *C. gestroi* may tunnel into the tough bark and sapwood of trees, potentially leading to circumferential debarking and subsequent tree mortality (Chouvenc and Foley 2018). As the extent of damage caused by termite feeding varies among trees, this may have implications for the community structure within forest ecosystems (Evans et al. 2019).

This study primarily employed 2D stress wave imaging techniques to assess the extent of termite-induced damage within the trunks of six trees. While using repeated stress wave tomography on living trees differs from previous methods that mainly relied on visual inspection of tree exteriors or observations of dead trees to investigate termites, the literature indicates that variations in termite species and environmental conditions can lead to different patterns of termite feeding (Scholtz et al. 2021).

Evans et al. (2019) observed that a higher occurrence of termites and the resulting damage to trees was associated with warmer and more humid climates. Other termite species, such as *Paraneotermes simplicicornis* (Banks), *Heterotermes aureus* (Snyder), and *C. formosanus*, exhibited increased rates of wood degradation with rising temperatures (Tai 2002). Therefore, warmer climates are often associated with higher termite frequencies and increased foraging frequency, a trend consistent with the findings of Chiu et al. (2015), who noted a significant positive correlation between temperature and termite foraging activity.

Our results showed that the damage rate caused by termite infestation was highest in tree specimens No. 28, 32, and 34, and that it typically occurred between June and August, which corresponded to the hottest season of the year, when termites would be most active. Taipei City experiences the highest average temperatures between June and September, ranging from approximately 28.3°C to 30.1°C, with relative humidities ranging from 70.2% to 75.3%. This result aligns with previous research findings (Chiu et al. 2015).

However, the maximum decay cavity rate due to termite infestation in Tree 29 and 43 occurred between February and April when Taipei City experiences the highest average relative humidity, approximately 74.9% to 77.8%, and temperatures ranging from 17.2 to 22.5 °C. This corresponds to the season immediately following the end of winter when temperatures begin to rise, and relative humidity is higher, potentially stimulating termite foraging activity. Therefore, the periods of higher termite infestation rates observed in this study mainly coincided with seasons characterized by higher temperatures and relative humidity, rather than during the colder winter months.

The pathways and methods of termite infestation in residential buildings can be categorized into “trail invasion” or “swarming invasion” (Yagi 2018). In trail invasion (by subterranean termite mud tunnels), termites nest in dead trees, standing trees, or underground, extend their trails to expand their damage range and gain access to buildings in ground contact. Trail invasion is a common mode of entry, where termite trails extend vertically from the ground upward. Swarming invasion (by aerial termite swarm flight) begins with winged termites swarming in pairs. They initially select damp nesting sites and later move to locations with relatively stable humidity, temperature, and a steady food supply (King and Spink 1969). This method may involve selecting trees, especially those with decayed portions, as these areas are conducive to termite concealment.

In this study, we observed that trees damaged by termites primarily experienced internal feeding within their trunks. Based on the initial damage locations and progression patterns, we inferred these two invasion modes in our study trees. The classification of termite infestation pathways into trail invasion (subterranean) or swarm invasion (aerial) in this study was primarily inferred based on the following criteria: (1) The primary vertical location of initial and most severe damage, damage concentrated at the base of the tree (e.g., 30 cm height) and progressing upwards, was indicative of subterranean trail invasion. Conversely, damage initiated at higher points on the trunk (e.g., >1m) and progressing downwards or localized in upper sections was considered indicative of aerial swarm invasion, potentially exploiting entry points like branch wounds. (2) Presence of external signs: while not always definitive, including visible mud tubes extending from the soil up the base

of the trunk supported classification as trail invasion. Direct evidence of aerial nests was not found, so swarm invasion was largely inferred from damage patterns inconsistent with a solely subterranean origin. The feeding pattern for subterranean trail invasions typically involved vertical extension from the tree base, followed predominantly by a circular direction, and finally, a radial path. This mode of infestation was often initiated by termite trails below the soil, initially invading the base of the tree and then progressing upward, classifying it as a subterranean termite trail invasion.

Another mode of infestation occurred when termites, after swarming, initially invaded a specific height on the tree and then moved downward towards the base. This mode was associated with alates and was categorized as an above-ground termite swarm invasion pattern.

During the inspection in August 2023, it was observed that Trees 29 and 32 still exhibited live termites, while Trees 28, 34, and 43 no longer showed signs of live termites. This phenomenon of termite disappearance from Trees 28, 34, 43 by August 2023 may have been influenced by physical disturbances during the inspection activities (e.g., drilling, sensor placement) or other environmental factors, potentially causing termite populations to vacate these specific locations between inspections.

The infestation mode for Trees 34 and 43 involved a termite swarm invasion pattern, which could make them susceptible to leaving the tree due to environmental disruptions. Whether the termite populations will return to these trees for feeding in the future requires further tracking and investigation.

Laboratory consumption rates of *Reticulitermes flaviceps* Oshima and *Nasutitermes parvonasutus* Light have been investigated on four different wood species (Tai 2002). Consumption rates ranged between 2.35 and 6.38 milligrams per day. Consumption rate of wood is influenced by several factors, including tree species, wood moisture content, termite colony condition, colony size, temperature, and humidity. It is noteworthy that these two termite species exhibited higher consumption rates on less dense wood species (Tai 2002).

Morales-Ramos and Rojas (2001) reported that laboratory feeding rate of the Formosan subterranean termite (*C. formosanus*) on Parana pine (*Araucaria angustifolia*), a highly preferred wood species, was approximately 0.49 milligrams per day. This rate was much lower than the rate reported by Tai (2002). In addition, a report by Jasmi and Ahmad (2011) mentions that hoop pines (*A. cunninghamii*), which have lower wood density, were attacked by *Coptotermes curvignathus* Holmgren, resulting in a damage rate of 15.9%. This accounted for 74% of the overall termite infestation rate (Jasmi and Ahmad 2011).

Secondary metabolites produced during wood decomposition may also influence interactions between termites and the wood. Therefore, variations in wood density and the production of secondary metabolites among different tree species result in different termite species showing preferences and ease of feeding on specific types of wood (Lai 2019).

Our study focused on hoop pine, *A. cunninghamii*, which is characterized by lower density, and we found that termites preferred less dense earlywood over latewood. Termites also initially targeted the sapwood/heartwood boundary. This behavior may be influenced by the secondary metabolites produced by living sapwood in the trees. Notably, termites were observed in our study to less frequently damage the sapwood region. Sapwood typically has higher moisture content, different chemical composition (e.g., fewer extractives, more starches) and is physiologically more active compared to heartwood (Li et al. 2019). These factors, or the proximity of sapwood to the external environment, might influence termite preference. Consequently, termites primarily consumed and extended their damage from the boundary between the sapwood and heartwood or the heartwood region, gradually progressing further into the heartwood.

The concept of tree defense known as the compartmentalization of decay in trees (CODIT) model, describes a self-protective system within trees where four conceptual zones—referred to as "reaction zones"—develop inside the wood to isolate and limit the spread of decay or injury (Morris et al. 2016; Pearce and Rutherford 1981; Shigo 1984; Smith 2020). In the first stage of the defense mechanism, physiological changes occur within the wood at Zones 1 (longitudinal), 2 (radial), and 3 (tangential). The final and strongest defense mechanism is the barrier zone produced by the formation of new tissue (Dunster et al. 2013). Typically, the direction in which decay in wood is most likely to expand follows a pattern of longitudinal first, then radial, and finally tangential. Visual inspection confirmed the localized internal decay zones observed in our acoustic data

In this research case, termites initially fed longitudinally, primarily along the tangential earlywood, and finally spread radially. This difference in feeding behavior compared to typical fungal decay spread patterns described by CODIT may be attributed to distinctions between active termite excavation and fungal decay processes. However, darker wood stains were observed near the wood surface affected by termite feeding

damage in the felled Tree 36 and noted in some endoscopic views. Wounding and subsequent microbial colonization, even if initiated by termites, can trigger CODIT responses in trees (Yatsko et al. 2024). This staining could therefore potentially represent a physiological response, such as the formation of a reaction zone (Wall 3 or even Wall 4, if cambial activity is involved) to internal wood damage and associated microbial activity caused or facilitated by termite feeding. Whether this observed staining fully aligns with defined CODIT walls would require further histological and chemical investigation for confirmation. It is important to note that while termite galleries represent a direct removal of wood, any associated staining or discoloration patterns would be the tree response to wounding and invasion by opportunistic microorganisms.

The generalizability of our findings may be constrained by the relatively small sample size. Although the trees were of a similar age range (40–50 years), variations in individual tree physiology, microclimate, and precise wood moisture content (which was not measured) could have influenced stress wave velocities and termite activity. We attempted to mitigate this by focusing on relative changes within individual trees. Furthermore, stress wave imaging possesses inherent resolution limitations. Previous research (Ostrovsky et al. 2017) indicated that stress wave technology only detected defects or decay when they occupied more than 2.8%–5% of the cross-sectional area, meaning that very small, isolated cavities or incipient decay might not be detected by this method. Accuracy can also be affected if the software does not adequately account for irregular trunk geometries. Species level identification of termite species was not possible for some trees where only remnant damage was present. Finally, the classification of infestation pathways was largely inferred from damage patterns rather than direct observation of alate colonization or extensive subterranean tunneling.

Conclusions

C. formosanus infested urban *A. cunninghamii* trees through both subterranean tunneling and aerial swarm invasions. Termite feeding damage was primarily concentrated in the heartwood, progressing longitudinally before moving tangentially through the preferred earlywood and then radially. Damage rates increased most substantially during warmer, humid seasons, with observed increases as high as 21% over a 2-month period. These findings demonstrate the value of repeated non-destructive stress wave imaging for monitoring the spatiotemporal dynamics of termite infestations, which is crucial for risk assessment and management of urban trees.

Acknowledgments

We would like to express our special thanks to National Taiwan Normal University for providing the project and financial support that enabled us to conduct the investigation on campus tree safety risks. The authors also gratefully acknowledge Professor Hou-Feng Li from National Chung Hsing University for his assistance in identifying the termite samples.

References

Allison RB, Wang X, Senalik CA (2020) Methods for nondestructive testing of urban trees. Forests 11(12):1341. https://doi.org/10.3390/f11121341.

Chiu CI, Li HF, Yeh HT, Tsai MJ (2015) Termite survey of Zelkova serrata plantations in moderate and low altitude areas of Taiwan. J Experiment Forest National Taiwan University 29(2):69–77. https://doi.org/10.6542/EFNTU.2015.29(2).1.

Chiu CI, Yeh HT, Yu JC, Li HF, Tsai MJ (2020) Termite occurrence on tree trunk affected by tree species, tree size, and its crown coverage. J Experiment Forest National Taiwan University 34(1):15–24. https://doi.org/10.6542/EFNTU.202003_34(1).0002.

Chouvenc T, Foley JR (2018) *Coptotermes gestroi* (Wasmann) (Blattodea [Isoptera]: Rhinotermitidae), a threat to the Southeastern Florida urban tree canopy. Fla Entomol 101(1):79–90. https://doi.org/10.1653/024.101.0115.

Dunster JA, Smiley ET, Matheny N, Lilly S (2013) Tree risk assessment manual. International Society of Arboriculture, Champaign. 198 p.

Evans TA, Forscher BT, Trettin CC (2019) Not just urban: The Formosan subterranean termites, *Coptotermes formosanus*, is invading forests in the Southeastern USA. Biol Invasions 21:1283–1294. https://doi.org/10.1007/s10530-018-1899-5.

FAKOPP (2020) Manual for the ArborSonic 3D Acoustic tomography. User's manual v6.5. 63pp.

Goh CL, Rahim RA, Rahiman MHF, Talib MTM, Tee ZC (2018) Sensing wood decay in standing trees: A review. Sensor Actuat A-Phys 269:276–282. https://doi.org/10.1016/j.sna.2017.11.038.

Jasmi AH, Ahmad AH (2011) Termite incidence on an Araucaria plantation forest in Teluk Bahang, Penang. Insects 2(4):469–474. https://doi.org/10.3390/insects2040469.

King EG Jr, Spink WT (1969) Foraging Galleries of the Formosan Subterranean Termite, *Coptotermes formosanus*, in Louisiana. Ann Entomol Soc Am 62:536–542. https://doi.org/10.1093/AESA/62.3.536.

Lee HF, Yeh HT, Wang YN, Tsai MJ (2011) Termite diversity and damage pattern in tropical botanical garden of Taiwan. J Experiment Forest National Taiwan University 25(2):139–147. https://doi.org/10.6542/EFNTU.201106_25(2).0005.

Li Y, Deng X, Zhang Y, Huang Y, Wang C, Xiang W, Xiao F, Wei X (2019) Chemical Characteristics of Heartwood and Sapwood of Red-Heart Chinese Fir (*Cunninghamia lanceolata*). For Prod J 69(2):103–109. https://doi.org/10.13073/FPJ-D-18-00042.

Li H, Zhang X, Li Z, Wen J, Tan X (2022) A review of research on tree risk assessment methods. Forests 13(10):1556. https://doi.org/10.3390/f13101556.

Lai, YY (2019) Termite infestation survey of protected old trees and baiting Formosan subterranean termite (Blattodea: Rhinotermitidae) in mango trees. National Chung Hsing University, master's thesis. 57 p. https://nchu.primo.exlibrisgroup.com/permalink/886NCHU_INST/2sntbr/alma990071951130107976

Liang WR, Maruyama M, Kanao T, Iwata R, Li HF (2020) Discovery of termitophilous rove beetles associated with Formosan subterranean termite *Coptotermes formosanus* in Taiwan, with the first larval description for

the tribe Termitohospitini (Coleoptera: Staphylinidae). Acta Entomologica Musei Nationalis Pragae, 60:77–87. https://doi.org/10.37520/aemnp.2020.005.

Lin CJ, Huang YH, Huang GS, Wu ML, Yang TH (2016) Detection of termite damage in hoop pine (*Araucaria cunninghamii*) trees by nondestructive techniques. J Trop For Sci 28(1):79–87. https://doi.org/10.6542/EFNTU.2015.29(2).2.

Lin WJ, Chen GY, Chiu CI, Liang WR, Tsai MJ, Yeh,HT, Li HF (2021) Damage and reinvasion of Asia subterranean termite on tree: A case study of Luchu Pine in Xiaping Tropical Botanical Garden. J Experiment Forest National Taiwan University 35(1):49–60. https://doi.org/10.6542/EFNTU.202103_35(1).0005.

Linhares CSF, Goncalves R, Martins LM, Knapic S (2021) Structural stability of urban trees using visual and instrumental techniques: a review. Forests 12(12):1752. https://doi.org/10.3390/f12121752.

Martiansyah I, Zulkarnaen RN, Hariri MR, Hutabarat PWK, Wardani FF (2022) Tree health monitoring of risking trees in the hotel open space: A case study in Rancamaya, Bogor. J Sylva Lestari 10(2):180–201. https://doi.org/10.23960/jsl.v10i2.570.

Morales-Ramos JA, Rojas MG (2001) Nutritional Ecology of the Formosan Subterranean Termite (Isoptera: Rhinotermitidae): Feeding Response to Commercial Wood Species. J Econ Entomol 94(2):516–523. https://doi.org/10.1603/0022-0493-94.2.516.

Morris H, Brodersen C, Schwarze FWMR, Jansen S (2016) The Parenchyma of Secondary Xylem and Its Critical Role in Tree Defense against Fungal Decay in Relation to the CODIT Model. Front Plant Sci 7. https://doi.org/10.3389/fpls.2016.01665.

Myer A, Forschler B (2018) Evidence for the Role of Subterranean Termites (*Reticulitermes* spp.) in Temperate Forest Soil Nutrient Cycling. Ecosystems 22:602–618. https://doi.org/10.1007/s10021-018-0291-8.

Ostrovsky R, Kobza M, Gazo J (2017) Extensively damaged trees tested with acoustic tomography considering tree stability in urban greenery. Trees 31:1015–1023. https://doi.org/10.1007/s00468-017-1526-6.

Pearce R, Rutherford J (1981) A wound-associated suberized barrier to the spread of decay in the sapwood of oak (*Quercus robur* L.). Physiol Plant Pathol 19:359–369. https://doi.org/10.1016/S0048-4059(81)80069-0.

Scholtz O, Knight M, Eggleton P (2021) Spatial structure of rainforest termites: Two matched pioneering cross-continental case studies. Biotropica, 53. https://doi.org/10.1111/btp.12959.

Shigo, AL (1984) Compartmentalization: a conceptual framework for understanding how trees grow and defend themselves. Annu Rev Phytopathol 22:189–214.

Smith K (2020) Whither compartmentalization of decay in trees? A commentary on: 'Using the CODIT model to explain secondary metabolites of xylem in defence systems of temperate trees against decay fungi'. Ann Bot 125(5):iv–vi. https://doi.org/10.1093/aob/mcaa035.

Soge AO, Popoola OI, Adetoyinbo AA (2021) Detection of wood decay and cavities in living trees: a review. Can J Forest Res 51(7):937–947. https://doi.org/10.1139/cjfr-2020-0340.

Tai WY (2002) Wood decomposition rates and caloric content changes of *Reticulitermes flaviceps* (Oshima) and *Nasutitermes parvonasutus* (Shiraki). National Taiwan University, master's thesis. 42 p. https://ntu.primo.exlibrisgroup.com/permalink/886NTU_INST/14poklj/alma991020160699704786

Thant, M., Lin, X., Atapattu, A., Cao, M., Xia, S., Liu, S, Yang X (2022) Activity-density and spatial distribution of termites on a fine-scale in a tropical rainforest in Xishuangbanna, southwest China. Soil Ecol Lett 5:169–180. https://doi.org/10.1007/s42832-022-0141-7.

Wei X, Du C, Xu S, Tian C, Yang X, Hu L, Pang P (2022) Research on stress wave wood nondestructive testing technology. J Phys Conf Ser 2366(1):012035. https://doi.org/10.1088/1742-6596/2366/1/012035.

Yagi H (2018) Study on the assessment of structural termite deterioration in building. National Taipei University of Technology, master's thesis. 147 p. https://hdl.handle.net/11296/ce8put

Yatsko AR, Wijas B, Calvert J, Cheesman AW, Cook K, Eggleton P, Gambold I, Jones C, Russell-Smith P, Zanne AE (2024) Why are trees hollow? Termites, microbes and tree internal stem damage in a tropical savanna. Funct Ecol 39:770–782. https://doi.org/10.1111/1365-2435.14727.